

Titanium Dioxide Nanosheets derived from Indonesian Ilmenite Mineral through Post- Hydrothermal Process

by Cek Turnitin

Submission date: 11-Dec-2022 10:36PM (UTC-0800)

Submission ID: 1978862284

File name: ndonesian_ilmenite_mineral_through_Post-Hydrothermal_Process.pdf (1.49M)

Word count: 3487

Character count: 19325

Titanium Dioxide Nanosheets derived from Indonesian Ilmenite Mineral through Post-Hydrothermal Process

Auzy, Ahmad

Department of Metallurgical and Materials Engineering, Faculty of Engineering, Universitas Indonesia

Latifa Hanum Lalarari

Metallurgical and Materials Research Center- Indonesia Institute of Science

Sofyan, Nofrijon

Department of Metallurgical and Materials Engineering, Faculty of Engineering, Universitas Indonesia

Ferdiansyah, Alfian

Department of Metallurgical and Materials Engineering, Faculty of Engineering, Universitas Indonesia

他

<https://doi.org/10.5109/4794174>

出版情報 : Evergreen. 9 (2), pp.470-475, 2022-06. 九州大学グリーンテクノロジー研究教育センター
バージョン :
権利関係 :



Titanium Dioxide Nanosheets derived from Indonesian Ilmenite Mineral through Post-Hydrothermal Process

Ahmad Fauzi^{1*}, Latifa Hanum Lalasari², Nofrijon Sofyan¹, Alfian Ferdiansyah¹,
Donanta Dhaneswar¹, Akhmad Herman Yuwono^{1*}

¹Department of Metallurgical and Materials Engineering, Faculty of Engineering, Universitas Indonesia,
Depok, 16424, Indonesia

²Metallurgical and Materials Research Center- Indonesia Institute of Science, Puspitek Serpong, South
Tangerang, Banten, 15314, Indonesia

¹⁴
*Author to whom correspondence should be addressed:
E-mail: ahmad.fauzi82@ui.ac.id, ahyuwono@eng.ui.ac.id

⁹
(Received February 11, 2022; Revised June 20, 2022; accepted June 20, 2022).

Abstract: Titanium dioxide (TiO₂) nanosheets are potential candidate material to be developed for photocatalytic applications. The natural resources of TiO₂ are abundant in the form of the mineral ilmenite (FeTiO₃). In this work, TiO₂ nanosheets have been synthesized using ilmenite mineral as the precursor through a post-hydrothermal process with temperature variations of 80, 100, 120, and 150°C for 24 hours. The resulting TiO₂ nanosheets were characterized by x-ray diffraction (XRD), scanning electron microscope (SEM) and ultraviolet visible-diffuse reflectance spectroscopy (UV-DRS). XRD analysis showed that the majority phase of the nanosheets was anatase TiO₂ accompanied by a small amount of sodium-titanate. The SEM study reveals the average thickness of nanosheets derived from post-hydrothermal process was 24.86 nm. XRD test results also showed that the increase in post-hydrothermal temperature from 80 to 150°C has resulted in an increase in the crystallite size of anatase TiO₂ from 35.14 to 45.59 nm. Such increase in the crystallite size has been found to lead to a decrease in the bandgap energy (E_g) of nanosheets from 2.85 to 2.70 eV. These results support the potential use of the resulting TiO₂ nanosheets as the photocatalytic material under the visible light illumination

Keywords: titanium dioxide nanosheets; ilmenite (FeTiO₃); optical properties

1. Introduction

Titanium dioxide (TiO₂) is found naturally in form of ilmenite mineral (FeTiO₃) with 30-65% content of TiO₂ and other oxide minerals^{1, 2}. However, this abundant ilmenite mineral is not currently optimized for use in various applications. This makes it necessary to process ilmenite further to obtain TiO₂ nanostructures. The structures at the nanometer level are assumed to have more pronounced properties than bulk materials. For several optical applications, nanoparticles³ or zero-dimensional (0-D) nanostructures still have limitations based on their low optical response to visible light that experience fast electron-hole pair recombination, thereby reducing photocatalytic efficiency^{4, 5}. Therefore, the modification of the TiO₂ morphology from zero-dimensional (0-D) to one-dimensional (1-D) structures needs to be carried out⁵ overcome the challenges⁶. One-dimensional (1-D) TiO₂ nanostructures such as nanowires, nanorods, nanotubes, and nanosheets are considered ideal for

⁵ photocatalytic applications. This is because they have a large surface area that can increase the absorption of photon energy in the visible light range, leading to more intensive interaction with the surrounding medium^{7, 8}.

The hydrothermal technique was used for the formation of the desired TiO₂ nanosheets because it is easy, inexpensive, and environmentally friendly^{9, 10}. Furthermore, it has the bandgap energy (E_g) closer to the TiO₂ bulk value of 3.20 eV, which facilitates the electron excitation under the visible light exposure¹¹ and enhances its photocatalytic performance

A previous study was carried out using the commercial precursor P25 Degussa nanoparticles to produce TiO₂ nanosheets¹². However, the bandgap energy of the nanosheets obtained was still significantly large at 3.65eV¹³, which is much higher than 3.20 eV of bulk TiO₂^{14, 15}. Therefore, the nanosheets were not suitable yet for the visible light photocatalysis application¹⁶. In addition, the P25 Degussa precursor material used has several obstacles such as the import routes, limited stock, and high price For a country like Indonesia which has

abundant mineral deposits, this motivates efforts to obtain an alternative TiO₂ precursor from the local resource, namely FeTiO₃ ilmenite mineral¹⁷⁾. A hydrometallurgical extraction process has also been carried out using the sulfate pathway as a route to convert the ilmenite into TiO₂¹⁸⁻²²⁾. In previous studies²³⁾, the extraction process has converted the ilmenite into filtrate and slag/residue. Meanwhile, this study was carried out systematically using the local Indonesia ilmenite slag as the precursor for the formation of TiO₂ nanosheets. The nanosheets obtained were further subjected to post-hydrothermal treatment with temperature variation. This is to enhance the nanocrystalline and reduce the bandgap energy close to the bulk value of anatase TiO₂ for fulfilling the requirement of the expected photocatalytic processes²⁴⁾.

2. Experimental

Titanate nanosheet was synthesized by hydrothermal method using local Indonesian mineral ilmenite (slag ilmenite resulting from sulfuric acid leaching process) as a precursor. The 10 grams of ilmenite slag was dispersed into 30 ml of 10 M sodium hydroxide (NaOH) solution. The mixed solution⁷⁾ was stirred for one hour to homogenize. Then the solution was transferred to a Teflon-coated autoclave. The autoclave was tightly closed and heated at 150°C for 24 h¹¹⁾ in the oven. After the autoclave was slowly cooled to room temperature, the powder product obtained was washed with distilled water, then¹²⁾ elled with 0.1 M hydrochloric acid (HCl), and finally washed with distilled water until the pH value of the treated nanosheets became neutral and dried at 110°C for 8 hours. Subsequently, post-hydrothermal treatment with varying temperatures (80, 100, 120, and 150°C) was given for 24 hours. For the purpose of post-hydrothermal treatment, TiO₂ nanosheets were placed on a buffer in a Teflon-coated autoclave to prevent the sample from being in direct contact with water such as cooking rice.

The resulting TiO₂ nanosheets were characterized using X-ray diffraction (B¹⁰⁾ or AXS-20 diffractometer using Cu K- α radiation of 1.5406 Å, operated at 40 kV, 40 mA). The size of the TiO₂ nanosheet crystallites was estimated using the Scherrer equation²⁵⁾

$$L = \frac{0.9 \lambda}{\beta \cos \theta} \quad (1)$$

where L is the mean crystal size,³⁾ λ is the X-ray wavelength, θ is the Br¹⁶⁾ angle, and β is the line widening, based on the fit¹⁹⁾ width at half maximum (FWHM) in radians²⁶⁾. The optical properties of the TiO₂ nanosheets were analyzed using UV-DRS spectrophotometer (UV-1601, Shimadzu). The bandgap energy (E_g) of TiO₂ nanosheets was estimated by analyzing the absorbance spectrum using Tauc plot method²⁷⁾. Further confirmation of the nanosheet

structure was carried out by observing using SEM (Leica Oxford Instrument, LEO 420i).

3. Result and Discussions

The increased temperature treatment in the post-hydrothermal process produced a dominant anatase phase followed by a minor sodium titanate phase. The anatase phase was formed when the temperature increased due to dehydration of the nanocrystalline Ti-OH interlayered group, leading to a Ti-O-Ti crystal structure²⁸⁾. In the process of forming the sodium titanate phase, the Ti-O-Ti bond formula occurs when hydrothermal treatment was carried out, where there are several bond chains of titanium with oxygen. Similarly, it also occurs in the TiO₂ anatase phase during a chain-breaking process to form a new structural phase with Ti-O-Na, Ti-OH bonds, while Na⁺ and H⁺ ions exchange take place when the process rises with HCl²⁹⁾. Figure 1 showed the XRD pattern for TiO₂ nanosheets that have passed through the post-hydrothermal treatment with temperature variations of 80, 100, 120, and 150°C. The results of the XRD analysis showed that an increase in the post-hydrothermal temperature of 150°C increases the diffraction intensity of TiO₂ anatase (○). This was indicated by a diffraction peak of 25.10° with a crystal plane (011). It was also discovered that there was an increase in the diffraction intensity of sodium titanate (▲) at 2θ , namely, 26.93, 34.03, and 52.01° with crystal planes (130), (140) and (440) according to the COD No. 1529535.

Based on Table 1, the relationship between crystall¹⁷⁾ size and post-hydrothermal temperature showed an increase in the crystallite size of the anatase phase on post-hydrothermal nanosheets. Furthermore, an increase in the diffraction peak's intensity in the XRD pattern showed that the TiO₂ nanocrystal grows more significantly from 35.14 to 45.59 nm. as post-hydrothermal temperature increases from 80 to 150°C

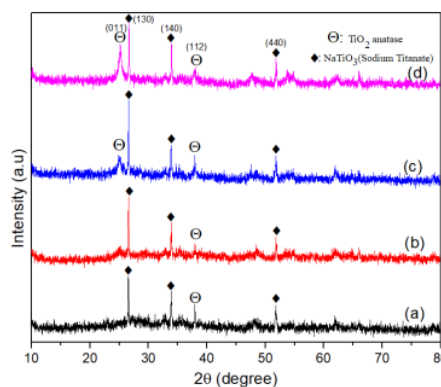


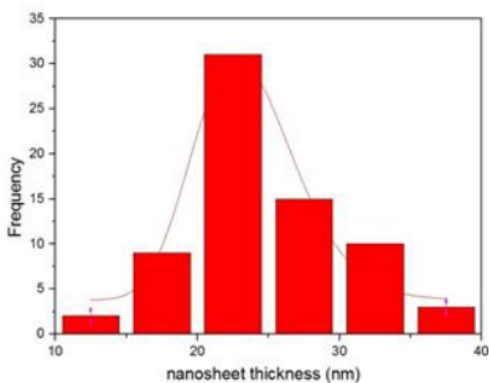
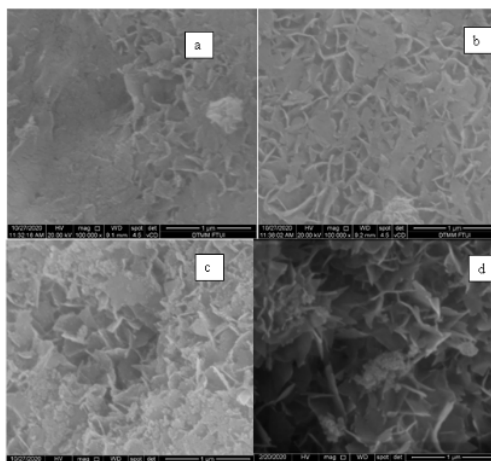
Fig. 1: XRD pattern of TiO₂ nanosheets at various post hydrothermal temperatures: (a) 80, (b) 100, (c) 120, and (d) 150°C

Table 1. The crystallite size of TiO₂ nanosheet after post-hydrothermal treatment

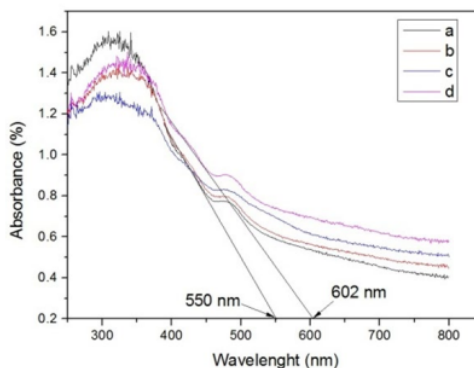
Code	Post-hydrothermal Temperature (°C)	Crystallite Size (nm)
Sample A	80	35.14
Sample B	100	40.26
Sample C	120	41.00
Sample D	150	45.59

The post-hydrothermal treatment formed the morphological integrity of the TiO₂ nanosheets structure as observed by SEM. The nanosheets structure occurred when TiO₂ crystals were treated with NaOH solution of high concentration, which turned titanate into layers and peels-off to form sheets. Furthermore, the nanosheets has a stable morphology due to the presence of a negatively charged Ti-O- bond and a positively charged Ti-bond on the side of the nanosheets. This makes it impossible for the titanate nanosheets to be rolled up to avoid the formation of nanotubes and maintain the integrity of the nanosheets. The TiO₂ nanosheets has an average thickness of 24.863 ± 0.355 nm and the thickness distribution of the nanosheets with R-Square = 0.88 as shown in Figure 2.

At a temperature of 80°C, the post-hydrothermal treatment showed that some of the nanosheets were not homogeneous and had not formed a perfect TiO₂ nanosheets (Fig.3a). Meanwhile, at 100°C, the morphological structure of titanium dioxide nanosheets looks like sheets that are more homogeneous and clearer (Fig.3b). At 120°C, it was discovered that the titanium dioxide nanosheets have cracked with several piles of powder on top of the nanosheets (Fig.3c). The increase in the temperature of post-hydrothermal treatment to 150°C has been found to be able to maintain the integrity of nanosheet structure and the morphology was homogeneous in a stable condition (Fig.3d).

Fig. 2: The thickness distribution of nanosheet TiO₂Fig. 3: SEM image of nanosheet TiO₂ at various post hydrothermal temperatures: (a) 80, (b) 100, (c) 120, and (d) 150°C

For determining the relationship between the crystallite size and optical properties of titanium dioxide nanosheets, UV-DRS spectroscopy was carried on the samples. The nanosheet samples show strong absorbance in the ultraviolet region (Fig. 4), while they are relatively transparent in the visible region. In addition, the absorption edges show red-shift from about 550 to 602 nm in wavelength as the post-hydrothermal temperature increased, which can be related to the lower bandgap energy (E_g) of TiO₂ nanosheets as estimated by the using the Tauc plot, which is plotted $(\alpha h\nu)^2$ as a function of photon energy ($h\nu$) given in Fig.5. Based on the results in Fig.5, it can be observed that with increasing post-hydrothermal treatment temperature from 80 to 150°C, the bandgap energy of TiO₂ nanosheets decreased from 2.85 to 2.70 eV.

Fig. 4: Absorbance spectra of TiO₂ nanosheet at various post hydrothermal temperatures: (a) 80, (b) 100, (c) 120, and (d) 150°C

The values are rather far below the bulk value of TiO₂ which is 3.20 eV. This can be due to impurities (Fe) in the TiO₂ nanosheet resulted from the nature of ilmenite (FeTiO₃). The presence of Fe element can indirectly acts as doping for anatase TiO₂ nanosheets. In addition, the crystallite size of TiO₂ nanosheets also influences the bandgap energy value. This showed that the larger the crystal size, the smaller the bandgap energy³⁰. It can be understood that increasing post-hydrothermal temperature in this work is useful for maintaining the structural integrity of TiO₂ nanosheets and facilitating lower bandgap energy so that the resulting nanosheets has the opportunity to be applied as photocatalytic material under the illumination of visible light.

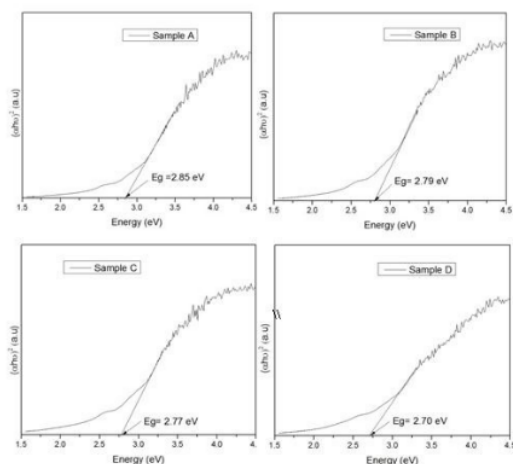


Fig. 5: Band gap energy of TiO₂ nanosheet at various post hydrothermal temperatures: (a) 80, (b) 100, (c) 120, and (d) 150°C

4. Conclusion

TiO₂ nanosheets have been successfully synthesized from a natural precursor of local Indonesian ilmenite at a low cost through a simple post-hydrothermal process. The XRD study revealed the presence of dominant TiO₂ anatase phase accompanied with small amount of sodium titanate. The post-hydrothermal treatment has succeeded in increasing the crystallite size of the anatase phase significantly from 35.14 to 45.59 nm and managed to maintain the integrity of the TiO₂ nanosheet structure. The increase in the crystallites size of the TiO₂ nanosheet has affected in the decrease in the bandgap energy from 2.85 to 2.70 eV. The resulting bandgap energy is lower than that of the bulk value of TiO₂ anatase which provides opportunities for the material to be used in the photocatalytic applications under visible light illumination.

4

Acknowledgements

The author is grateful to the Directorate of Research

and Development Universitas Indonesia for funding this study through the International Indexed Publication Grant (PUTI Doktor 2020) 2020 b201 on Agreement/contract number Number: BA-829/UN2.RST / PPM. 00.03.01 / 2020.

References

- 1) S. Samal, B. Mohapatra, and P. Mukherjee, "The effect of heat treatment on titania slag," *J. Minerals and Materials Characterization and Engineering.*, **9** (09)795(2010) .<https://www.scirp.org/html/20781.htm>
- 2) K. Taira, and H. Einaga, "Distribution Ratio of Pt on Anatase and Rutile TiO₂ Particles, Determined by X-ray Diffraction and Transmission Electron Microscopy Analysis of Pt/TiO₂ (P25)," *Evergreen.*, **5**(4)13-17(2018).doi:<https://doi.org/10.5109/2174853>.
- 3) A.C. Opia, M.K.A. Hamid, S. Syahrullail, C.A. Johnson, A.B. Rahim, and M.B. Abdulrahman, "Nano-Particles Additives as a Promising Trend in Tribology: A Review on their Fundamentals and Mechanisms on Friction and Wear Reduction." *Evergreen.*, **8**(4)777-798(2021).doi:<https://doi.org/10.5109/4742121>.
- 4) D. Chen, Y. Chen, N. Zhou, P. Chen, Y. Wang, K. Li, S. Hou, P. Chwng, P. Peng, R. Zhang, L. Wang, H. Liu, Y. Lu, and R. Ruan, "Photocatalytic degradation of organic pollutants using TiO₂-based photocatalysts: A review," *J. of Cleaner. Production.*, **268** 121725 (2020). doi: <https://doi.org/10.1016/j.jclepro.2020.121725>.
- 5) I.H. Dwirekso, and S.M. Ibadurrohman, "Synthesis of TiO₂-SiO₂-CuO Nanocomposite Material and Its Activities for Self-cleaning," *Evergreen.*, **7**(02) 285-291(2020).doi:<https://doi.org/10.5109/4055234>.
- 6) S. Reghunath, D. Pinheiro, and S.D. KR, "A review of hierarchical nanostructures of TiO₂: Advances and applications," *Applied Surface Science Advances.*, **3** 100063(2021).doi:<https://doi.org/10.1016/j.apsadv.2021.100063>
- 7) J. Tian, Z. Zhao, A. Kumar, R.I. Boughton, and H. Liu, "Recent progress in design, synthesis, and applications of one-dimensional TiO₂ nanostructured surface heterostructures: a review," *Chem.Soc.Rev.*, **43**(20) 6920-6937 (2014). doi: 10.1039/C4CS00180J.
- 8) A. Azani, D.S.C. Halin, M.M.A.F. Abdullah, and K.A. Razak, "The Effect of GO/TiO₂ Thin Film During Photodegradation of Methylene Blue Dye," *Evergreen.*, **8** (03) 556-564 (2021).doi:<https://doi.org/10.5109/4491643>.
- 9) L. Lai, E. Lei, C. hu, D. Zhao, W. Zhao, Z. Guo, and D. Huang, "A facile hydrothermal synthesis and properties of TiO₂ nanosheet array films," *Mater. Res. Express.*, **7** (1) 015053 (2020).doi:<https://doi.org/10.1088/2053-1591/ab638>

- b.
- 10) Z.F. Zahara, "Economic assessment of the sugarcanebased bio-refinery in indonesia," *Evergreen.*, **5** (2) 67– 77 (2018).
 - 11) N.I.I. Zamri, S.L.N Zulmajdi, E.Kusrini, K. Ayuningtyas, H.M. Yasin, and A. Usman, "Rhodamine B Photocatalytic Degradation using CuO Particles under UV Light Irradiation for Applications in Industrial and Medical Fields." *Evergreen.*, **7** (2) 280-284 (2020). doi: <https://doi.org/10.5109/4055233>.
 - 12) F. Chen, P. Fang, Y. Gao, Z. Liu, and Y. Dai, "Effective removal of high-chroma crystal violet over TiO₂-based nanosheet by adsorption-photocatalytic degradation," *Chemical Engineering Journal.*, **204** 107-113 (2012). doi: <https://doi.org/10.1016/j.cej.2012.07.030>.
 - 13) L. Sheng, T. Liao, L. Kou, and Z.Sun, "Single-crystalline ultrathin 2D TiO₂ nanosheets: a bridge towards superior photovoltaic devices," *Materials Today Energy.*, **3** 32-39 (2017). doi: <https://doi.org/10.1016/j.mtener.2016.12.004>.
 - 14) C. Kormann, D.W. Bahnemann, and M.R. Hoffmann, "Preparation and characterization of quantum-size titanium dioxide," *J.Phys. Chem.*, **92**(18) 5196-5201 (1988). doi: <https://doi.org/10.1021/j100329a027>.
 - 15) M. Ezaki, and K. Kusakabe, "Highly Crystallized Tungsten Trioxide Loaded Titania Composites prepared by Using Ionic Liquids and their Photocatalytic Behaviors," *Evergreen.*, (2014). doi: <https://doi.org/10.5109/1495159>.
 - 16) A.S. Idris, S. Ghosh, and K. Hamamoto, "A multi-layer stacked all sol-gel fabrication technique for vertical coupled waveguide," *Evergreen.*, **7**(2) 280-284 (2020). doi:<https://doi.org/10.5109/4055233>.
 - 17) T.H. Nguyen, and M.S. Lee, "A review on the recovery of titanium dioxide from ilmenite ores by direct leaching technologies," *Mineral Processing and Extractive Metallurgy Review.*, **40**(4) 231-247 (2019).doi:<https://doi.org/10.1080/08827508.2018.1502668>.
 - 18) Y. Liu, T. Qi, J. Chu, Q. Tong, Yi. Zhang, "Decomposition of ilmenite by concentrated KOH solution under atmospheric pressure," *Int. J. Miner. Process.*, **81**(2) 79-84 (2006). doi: <https://doi.org/10.1016/j.minpro.2006.07.003>.
 - 19) L.H. Lalasari, R. Subagja, A.H.Yuwono, F. Firdiyono, S. Harjanto, and B. Suharno, "Sulfuric Acid Leaching of Bangka Indonesia Ilmenite Ore and Ilmenite Decomposed by NaOH," *Advanced Materials Research.*, (2013). doi: <https://doi.org/10.4028/www.scientific.net/AMR.789.522>.
 - 20) L.H. Lalasari, R. Subagja, A.H.Yuwono, F. Firdiyono, S. Harjanto, and B. Suharno, "Preparation, Decomposition and Characterizations of Bangka-Indonesia Ilmenite (FeTiO₃) derived by Hydrothermal Method using Concentrated NaOH Solution," *Advanced Materials Research.*, (2012). doi:<https://doi.org/10.4028/www.scientific.net/AMR.535-537.750>.
 - 21) L.H Lalasari, F. Firdiyono, L. Andriyah, A. Suharyanto, T. Arini, A. Ridhova, and N.C. Natasha, "The dissolution of cassiterite Indonesia using hydrometallurgical process in the aerated reactor," *AIP.Conf.Proc.*, (2020). doi: <https://doi.org/10.1063/5.0002208>.
 - 22) A.Fauzi, L.H. Lalasari, N. Sofyan, D. Dhaneswara and A. H. Yuwono, "Synthesis of titanium oxysulfate from ilmenite through hydrothermal, water leaching and sulfuric acid leaching routes," *AIP.Conf.Proc.*,(2020).doi:<https://doi.org/10.1063/5.0015864>.
 - 23) H.Latif, A.H. Yuwono, F. Firdiyono, N.T. Rochman, S. Harjanto, B. Suharno, "Controlling the Nanostructural Characteristics of TiO₂ Nanoparticles Derived from Ilmenite Mineral of Bangka Island through Sulfuric Acid Route," *Applied Mechanics and Materials.*, (2013). doi: <https://doi.org/10.4028/www.scientific.net/amm.391.34>.
 - 24) A.H.Yuwono, N. Sofyan, I. Kartini, A.Ferdiansyah. T.H. Pujianto, "Nanocrystallinity enhancement of TiO₂ nanotubes by post-hydrothermal treatment," *Advanced Materials Research.*, (2011). doi: <https://doi.org/10.4028/www.scientific.net/AMR.277.90>.
 - 25) Cullity, B.D, "Elements of X-ray Diffraction," *Addison-Wesley Publishing.*, (1956). <http://117.239.25.194:7000/jspui/bitstream/123456789/954/1/preliminary%20and%20content.pdf>
 - 26) C. Suryanarayana, and M.G. Norton, "X-ray diffraction: a practical approach," *Springer Science & Business Media.*,1998. https://books.google.co.id/books?hl=id&lr=&id=u7ezrnw3_tgc&o.
 - 27) J. Tauc, R. Grigorovici, and A. Vancu, "Optical properties and electronic structure of amorphous germanium," *phys.stat.sol.*,**15**(2) 627-637 (1966).doi:<https://doi.org/10.1002/pssb.19660150224>.
 - 28) S.Rashad, A. Zaki, and A. Farghali, "Morphological effect of titanate nanostructures on the photocatalytic degradation of crystal violet," *Nanomaterials and Nanotechnology.*, **9** 1847980418821778 (2019). doi: <https://doi.org/10.1177/1847980418821778>.
 - 29) J.Yang, Z. Jin. X. Wang.W. Li, J. Zhang, S. Zhang, X.Guo, and Z. Zhang, "Study on composition, structure and formation process of nanotube Na₂Ti₂O₄(OH)," *Dalton.Trans.*, **20** 3898-3901(2003).doi:<https://doi.org/10.1039/B305585J>.

- 30) A.H.Yuwono, B. Liu, J. Xue, J.Wang, H.I. Elim, W. Ji, Y.Li and T.J. White, "Controlling the crystallinity and nonlinear optical properties of transparent TiO₂-PMMA nanohybrids," *J. Mater. Chem.*, **14**(20) 2978-2987(2004).doi:<https://doi.org/10.1039/b403530e>

Titanium Dioxide Nanosheets derived from Indonesian Ilmenite Mineral through Post-Hydrothermal Process

ORIGINALITY REPORT

12%

SIMILARITY INDEX

6%

INTERNET SOURCES

10%

PUBLICATIONS

3%

STUDENT PAPERS

PRIMARY SOURCES

- 1** Submitted to Universitas Jenderal Soedirman 2%

Student Paper
- 2** Şevket Onur Kalkan, Ahmet Yavaş, Saadet Güler, Merve Torman Kayalar, Mücahit Sütçü, Lütfullah Gündüz. "An experimental approach to a cementitious lightweight composite mortar using synthetic wollastonite", Construction and Building Materials, 2022 1%

Publication
- 3** www.iieta.org 1%

Internet Source
- 4** Ike Iswary Lawanda. "The importance of information access of cultural values to the principles of sustainable development in climate change", Global Knowledge, Memory and Communication, 2019 1%

Publication
- 5** Shalini Reghunath, Dephan Pinheiro, Sunaja Devi KR. "A review of hierarchical nanostructures of TiO₂: Advances and 1%

applications", Applied Surface Science
Advances, 2021

Publication

6	cancerres.unboundmedicine.com Internet Source	1 %
7	Yongxia Li, Binsheng Yang, Bin Liu. "Synthesis of BiVO ₄ nanoparticles with tunable oxygen vacancy level: The phenomena and mechanism for their enhanced photocatalytic performance", Ceramics International, 2021 Publication	1 %
8	hal.archives-ouvertes.fr Internet Source	1 %
9	Jindong Zhang, Chongzhi Wu. "Technical Evaluation Method of Mechanical Equipment Item Substitution in the Procurement and Construction Process of Nuclear Power Plant", Journal of Nuclear Engineering and Radiation Science, 2022 Publication	<1 %
10	Yuwono, Akhmad Herman, Binghai Liu, Junmin Xue, John Wang, Hendry Izaac Elim, Wei Ji, Ying Li, and Timothy John White. "Controlling the crystallinity and nonlinear optical properties of transparent TiO ₂ –PMMA nanohybrids", Journal of Materials Chemistry, 2004. Publication	<1 %

11

Samapti Kundu, Biswarup Satpati, Tanusree Kar, Swapan Kumar Pradhan. "Microstructure characterization of hydrothermally synthesized PANI/V₂O₅·nH₂O heterojunction photocatalyst for visible light induced photodegradation of organic pollutants and non-absorbing colorless molecules", Journal of Hazardous Materials, 2017

Publication

<1 %

12

Goa, Y.. "Controlled detitanation of ETS-10 materials through the post-synthetic treatment and their applications to the liquid-phase epoxidation of alkenes", Microporous and Mesoporous Materials, 20040521

Publication

<1 %

13

Liu, Y.. "Decomposition of ilmenite by concentrated KOH solution under atmospheric pressure", International Journal of Mineral Processing, 200611

Publication

<1 %

14

Po-Tsung Hsiao. "Coordination of Ti⁴⁺ Sites in Nanocrystalline TiO₂ Films Used for Photoinduced Electron Conduction: Influence of Nanoparticle Synthesis and Thermal Necking", Journal of the American Ceramic Society, 04/2009

Publication

<1 %

15	ejournal2.undip.ac.id Internet Source	<1 %
16	psecommunity.org Internet Source	<1 %
17	Hsiao, P.T.. "Nanocrystalline anatase TiO ₂ derived from a titanate-directed route for dye-sensitized solar cells", Journal of Photochemistry & Photobiology, A: Chemistry, 20070430 Publication	<1 %
18	Piyumi Kodithuwakku, Dilushan Jayasundara, Imalka Munaweera, Randika Jayasinghe et al. "A Review on Recent Developments in Structural Modification of TiO ₂ For Food Packaging Applications", Progress in Solid State Chemistry, 2022 Publication	<1 %
19	repositorio.ufscar.br Internet Source	<1 %
20	Helmiyati Helmiyati, Zahra Shabira Zakiyah Hidayat, Ida Frisca Royani Sitanggang, Dyah Liftyawati. "Antimicrobial packaging of ZnO-Nps infused into CMC-PVA nanocomposite films effectively enhances the physicochemical properties", Polymer Testing, 2021 Publication	<1 %

21

Arlina Prima Putri, Rizna Triana Dewi, Aniek Sri Handayani, Sri Harjanto, Mochamad Chalid.
"Screening of proteins based on macro-algae from West Java coast in Indonesian marine as a potential anti-aging agent", AIP Publishing, 2018

Publication

<1 %

Exclude quotes On

Exclude matches Off

Exclude bibliography On